

Supporting Information for

Structural and Magnetic Investigations of a Binuclear Coordination Compound of Dysprosium (III) Dinitrobenzoate .

Balkaran Singh Sran,^a Jessica Flores Gonzalez,^b Vincent Montigaud,^b Boris Le Guennic,^b Fabrice Pointillart*,^b Olivier Cador*,^b Geeta Hundal*^a

^a Department of Chemistry, UGC sponsored centre of advance studies-II, Guru Nanak Dev University, Amritsar-143005, Punjab, India.

^b Univ Rennes, CNRS, ISCR (Institut des Sciences Chimiques de Rennes) - UMR 6226, 35000 Rennes, France.

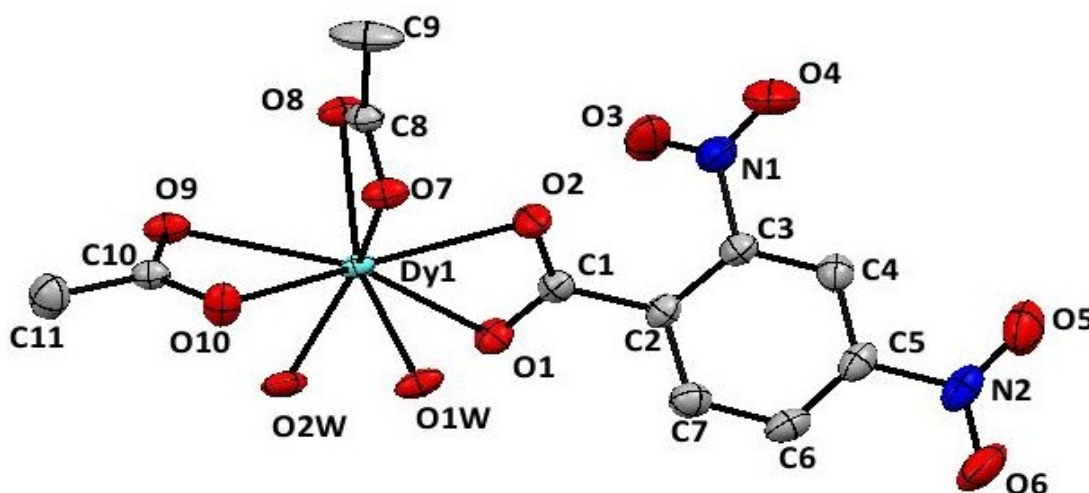


Fig. S1 ORTEP diagram showing asymmetric unit of Dy complex with 40 % ellipsoid probability. Hydrogen atoms are omitted for clarity

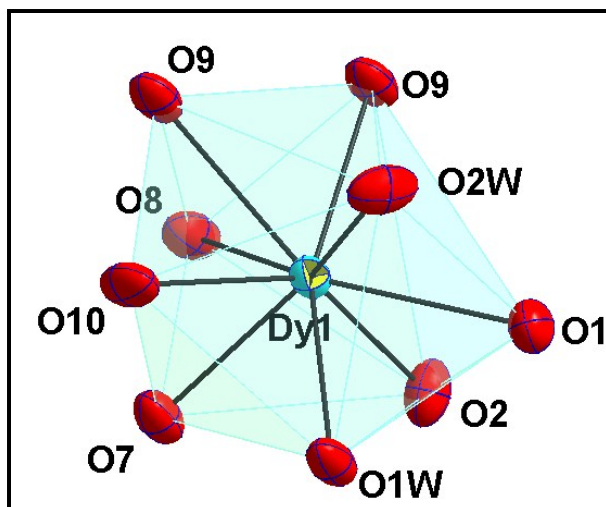


Fig. S2 Showing the Polyhedron around the metal ion.

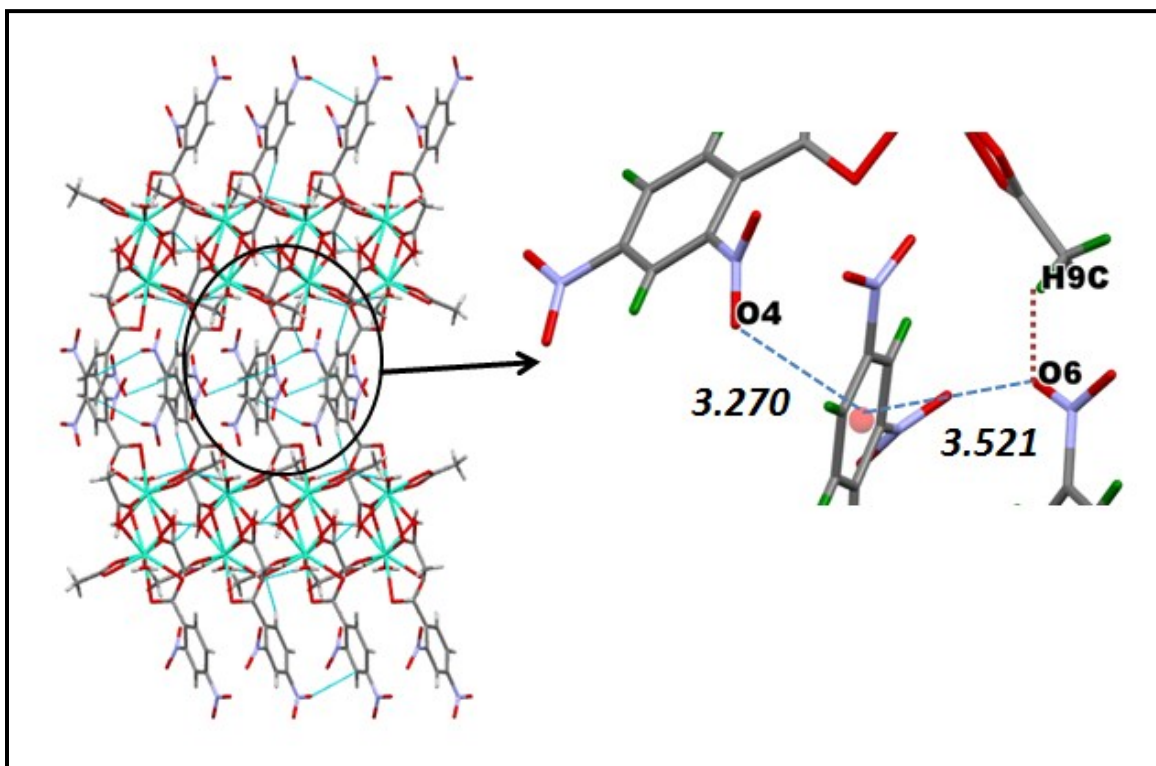


Fig.S3 Showing intermolecular hydrogen bonding (dotted magenta coloured line) and Lone pair-- π interactions (dotted blue coloured line) between different chains along a axis (bc plane).

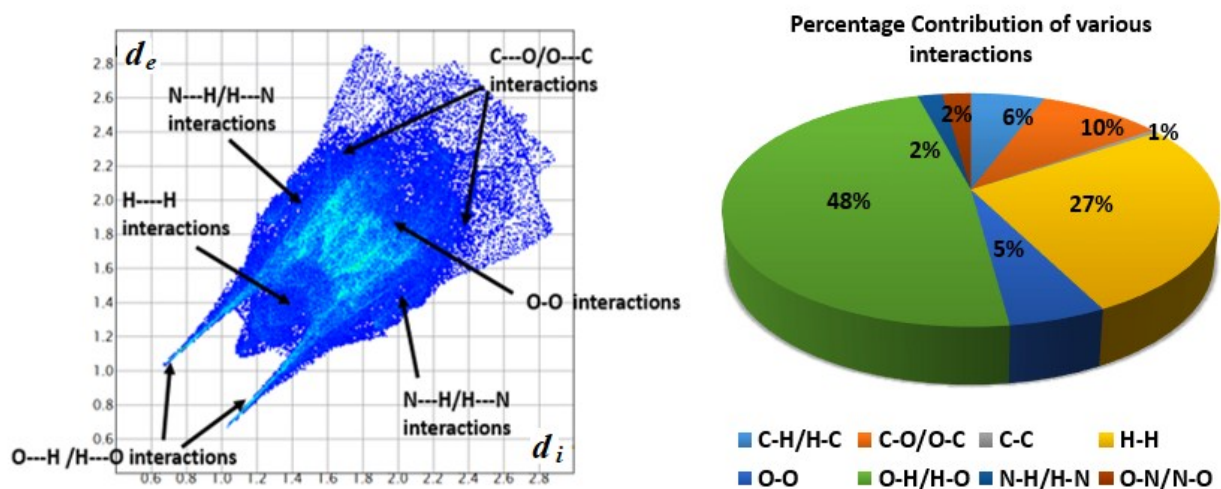


Fig. S4 2D fingerprint plots for **1**, d_e and d_i are the distances to the nearest atom centre exterior and interior to the surface, respectively (left). Pie plot showing percentage share of various interactions to the Hirshfeld surface (right).

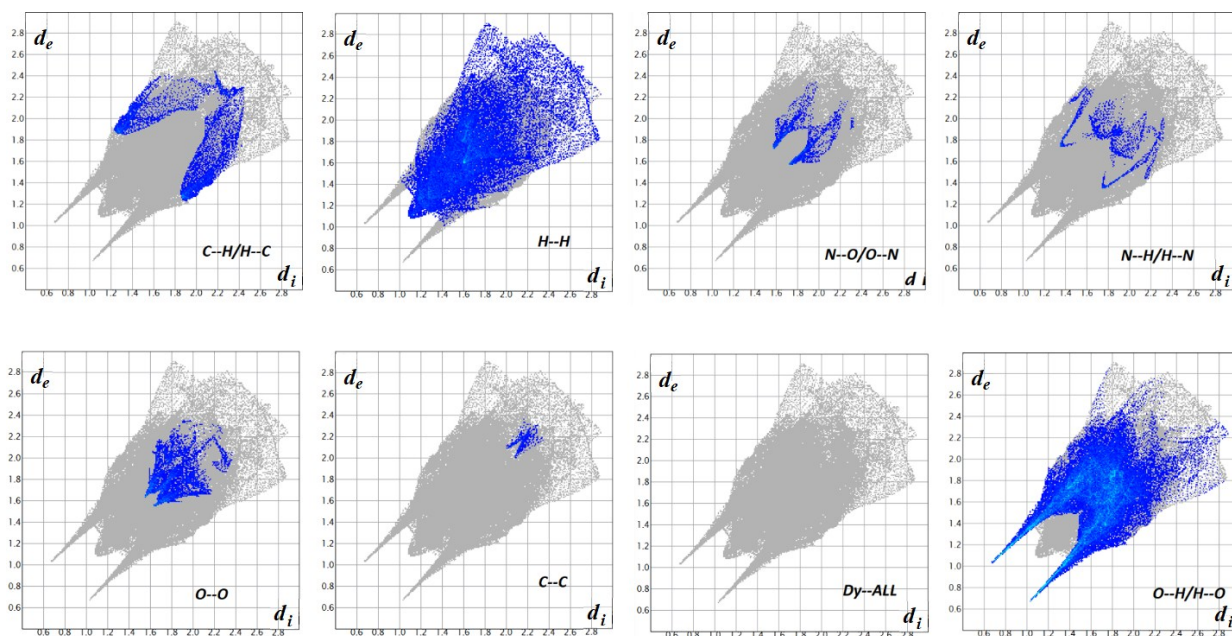


Fig. S5 Fingerprint plots of C-H/H-C, H-H, N-O/O-N, N-H/H-N, O-O, C-C, Dy-All and O-H/H-O pairs. The grey shadow outlines the total fingerprint in **1**.

IR Spectroscopy

The IR spectrum of **1** shows a band for OH at 3348 cm^{-1} , characteristic peaks of asymmetric and symmetric stretches of COO^- at 1546 cm^{-1} and 1377 cm^{-1} , respectively. $\Delta\nu = \nu_{\text{asym}}(\text{COO}^-) - \nu_{\text{sym}}(\text{COO}^-)$ is less than 200 cm^{-1} which clearly indicates that ligand binds with the metal centre in a bidentate chelate mode.¹ The compound contains an aromatic N-O stretch around 1349 cm^{-1} and a weak band around 617 cm^{-1} that is assigned to M-O vibrations (Fig. S7).

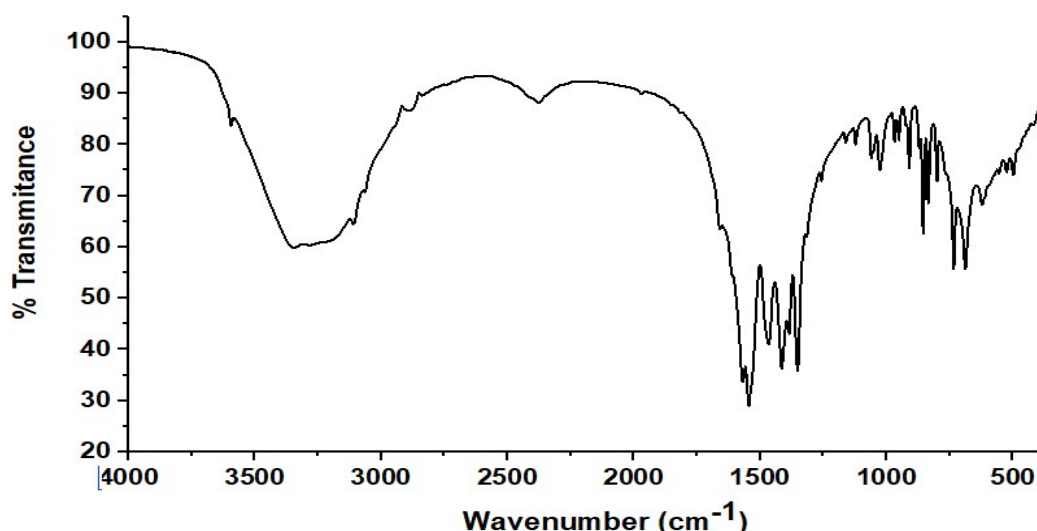


Fig. S6 IR spectra of complex **1**.

- 1 M. I. Azócar, H. Muñoz, P. Levin, N. Dinamarca, G. Gómez, A. Ibañez, M. T. Garland and M. A. Paez, *Commun. Inorg. Synth.* 2013, **1**, 19-21.

Thermogravimetric analysis

The thermal stability of Dy (III) complex was examined by TGA (Fig. S8). In a general manner, Complex loses four coordinated water molecules between 120 and $183\text{ }^\circ\text{C}$, endothermically (calculated weight loss, 6.7% ; observed weight loss, 6.2%). Beyond this temperature there is a weight loss between 254°C and 418°C corresponding to the loss of DNB molecules (Calculated weight loss, 39.8% ; observed weight loss, 40.2%), remaining organic part is lost up to $800\text{ }^\circ\text{C}$ leaving behind Dy_2O_3 (35.8%) as residue.

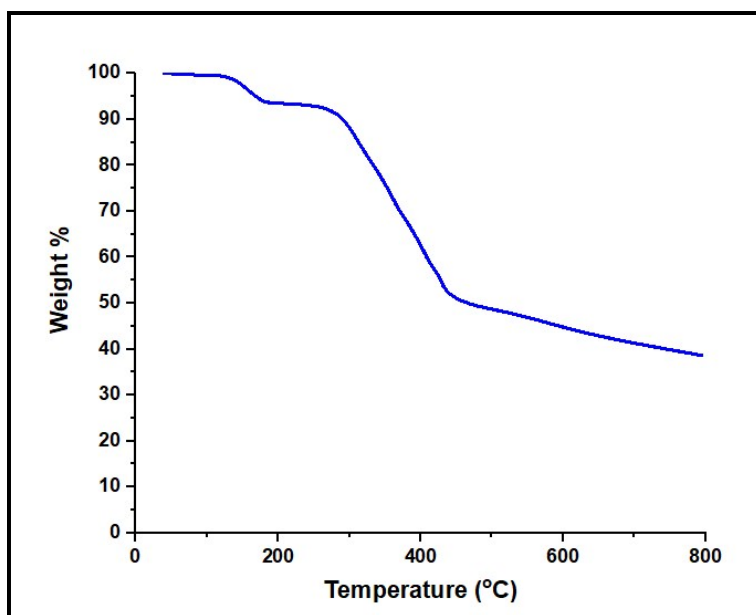


Fig. S7 TGA analysis for **1**.

Powder X-ray Diffraction studies

In order to confirm that the single crystal structure of compounds **1** corresponds to the bulk material as well as its phase purity, the powder X-ray data were recorded at room temperature. The experimental and simulated (from the single crystal data) patterns are shown in Fig. S6, providing a very good match between the two.

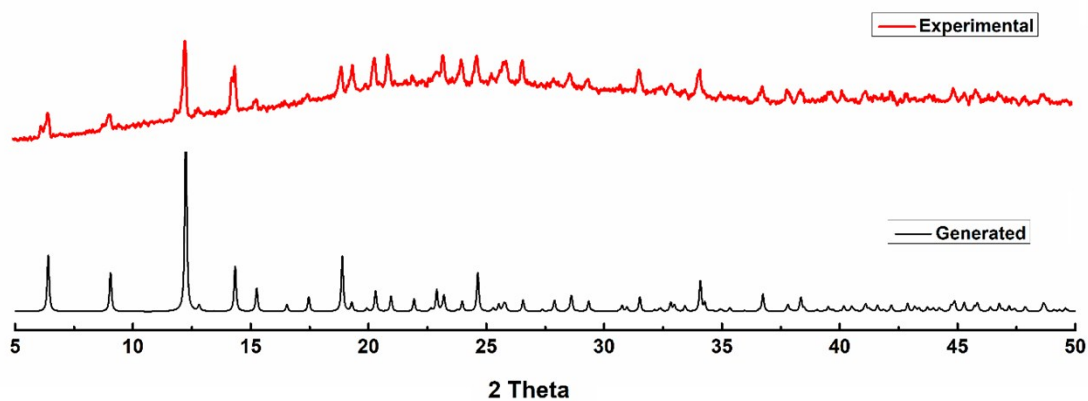


Fig. S8 Generated (black) and experimental (red) PXRD spectrum of complex **1**

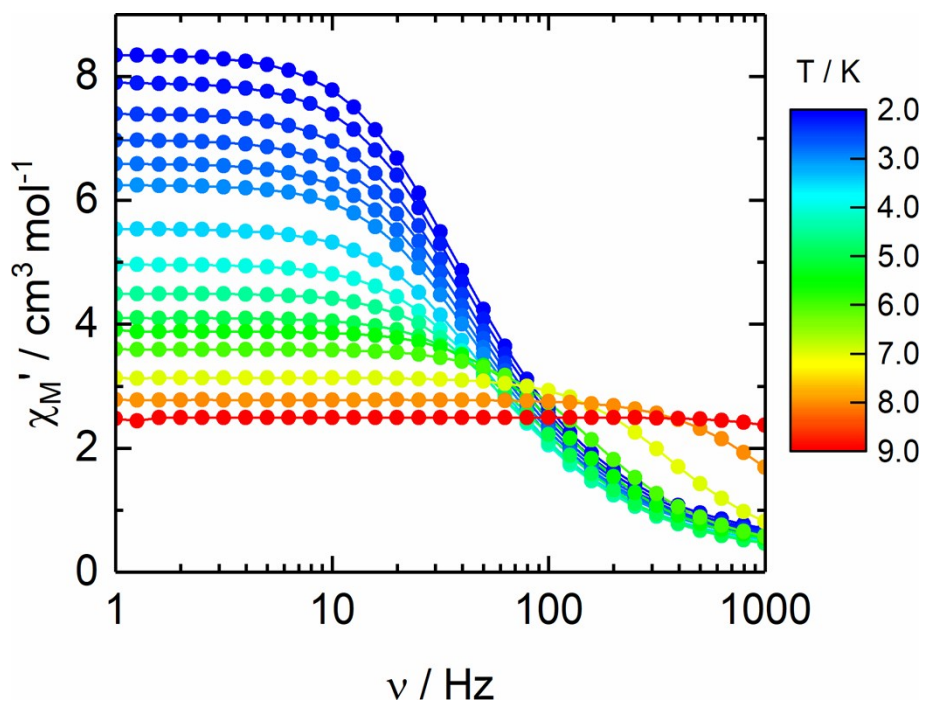


Fig. S9 Frequency dependence of χ_M' of **1** from 2 to 15K under zero- applied magnetic field.

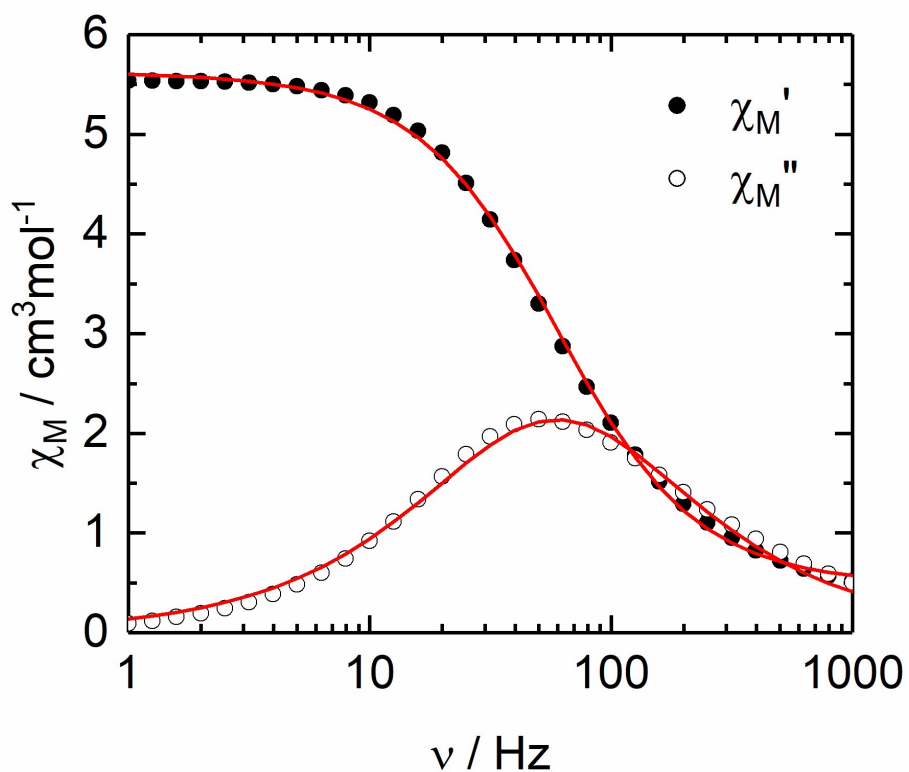


Fig. S10 Frequency dependence of the in-phase (χ_M') and out-of-phase (χ_M'') components of the ac susceptibility measured on powder at 3.5 K in zero dc field with the best fitted curves (red lines) for **1** with the extended Debye model (see below).

Extended Debye model.

$$\chi_M' = \chi_s + (\chi_T - \chi_s) \frac{1 + (\omega\tau)^{1-\alpha} \sin\left(\alpha \frac{\pi}{2}\right)}{1 + 2(\omega\tau)^{1-\alpha} \sin\left(\alpha \frac{\pi}{2}\right) + (\omega\tau)^{2-2\alpha}}$$

$$\chi_M'' = (\chi_T - \chi_s) \frac{(\omega\tau)^{1-\alpha} \cos\left(\alpha \frac{\pi}{2}\right)}{1 + 2(\omega\tau)^{1-\alpha} \sin\left(\alpha \frac{\pi}{2}\right) + (\omega\tau)^{2-2\alpha}}$$

With χ_T the isothermal susceptibility, χ_s the adiabatic susceptibility, τ the relaxation time and α an empiric parameter which describe the distribution of the relaxation time. For SMM with only one relaxing object α is close to zero. The extended Debye model was applied to fit simultaneously the experimental variations of χ_M' and χ_M'' with the frequency ν of the oscillating field ($\omega = 2\pi\nu$). Typically, only the temperatures for which a maximum on the χ_M'' vs. ν curves, have been considered (see Fig. S10 for an example). The best fitted parameters τ , α , χ_T , χ_s in the range 2-7 K are listed in Table S4 with the coefficient of determination R^2 .

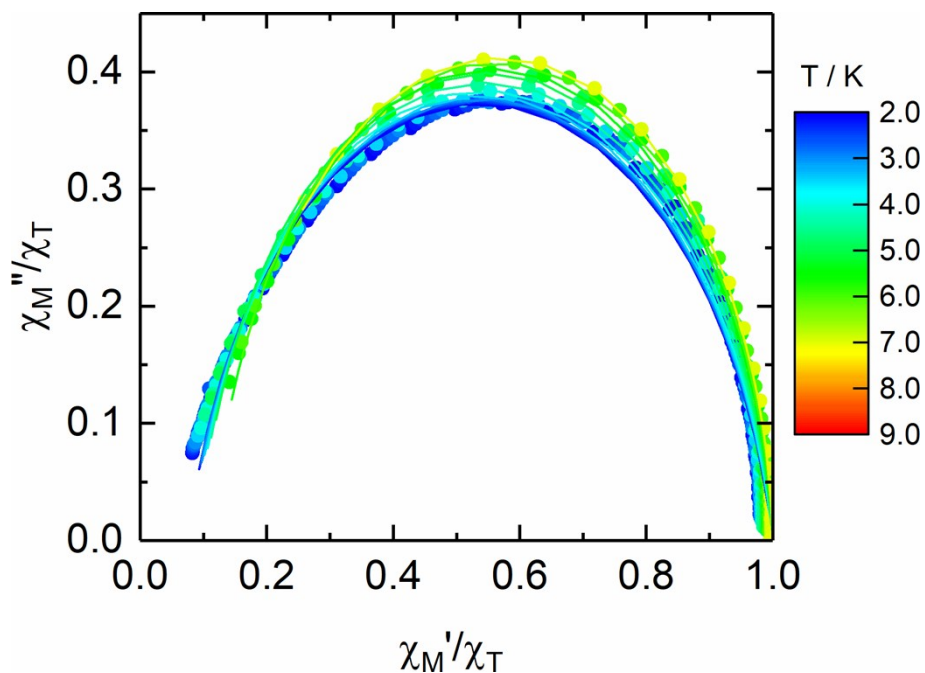


Fig. S11 Normalized Cole-Cole plots for **1** at several temperatures between 2 and 7K.

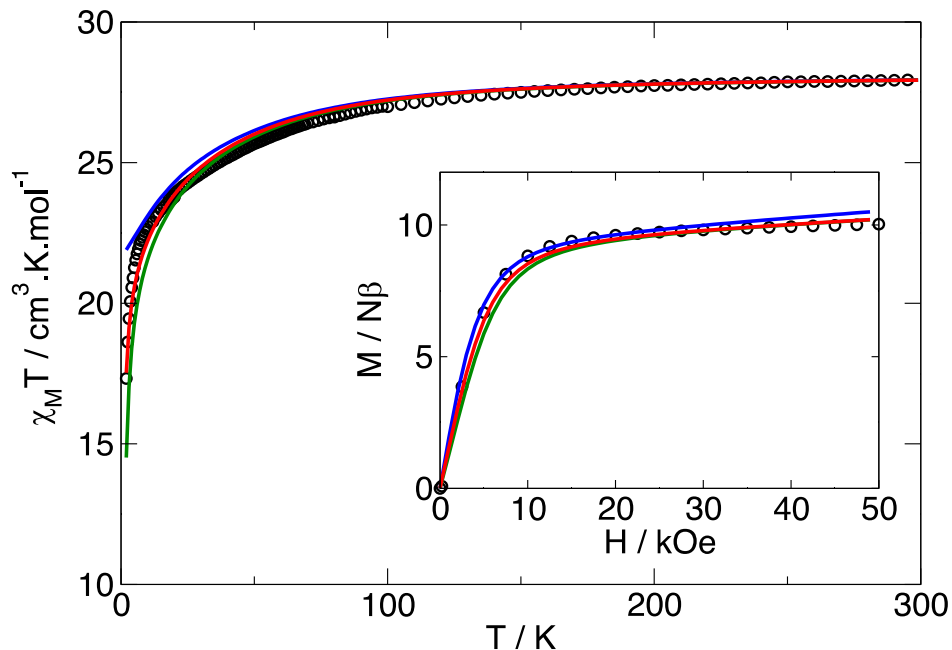


Fig. S12 Thermal evolution of the molar magnetic susceptibility in function of the temperature and M vs H curves at 2 K (inset) for **1**. The dark dots represent experimental results while solid lines correspond to calculated data considering isolated Dy centers (blue), only the dipolar interactions (green) and both dipolar and exchange contributions for a fitting exchange term $J^{\text{exch}} = 0.04 \text{ cm}^{-1}$, in the Lines model (red).

Mapping of the molecular electrostatic potential.

The molecular electrostatic potential is mapped and represented using the home-made **CAMMEL** code (**C**ALculated **M**olecular **M**ultipolar **E**lectrostatics).

$$V(r_i) = \sum_i^N \frac{q_i}{|r_i - r|} + \frac{p_i \cdot r_i}{|r_i - r|^3} + \frac{r_i \cdot (Q_i \times r_i)}{|r_i - r|^5}$$

where q_i , p , Q_i are respectively the charge, dipole and quadrupole moments of the i -th atom. The potential is drawn on a sphere defined by the user around the central lanthanide ion, for a given state (ground state in this case). For a clearer representation of the potential, the intensity can be directly related to both the color (red = high potential and blue = low potential) and the height of the irregularities.

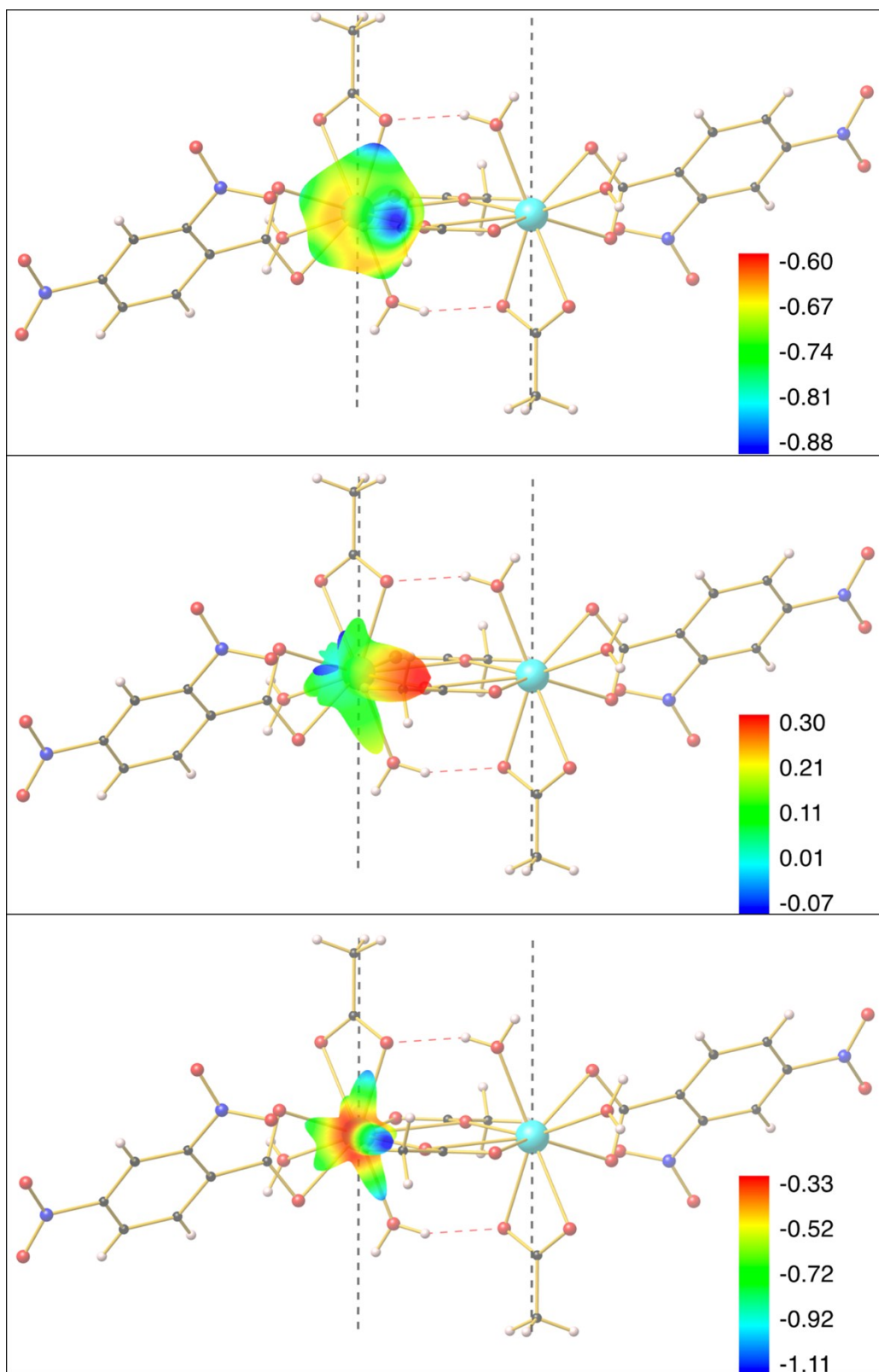


Fig. S13 Representation of the charge (top), dipole (middle) and quadrupole (bottom) components of the electrostatic potential mapped around one of the magnetic center.

Table S1. Selected bond lengths and angles for **1**.

O1 -Dy1	2.475(2)
O2 -Dy1	2.472(2)
O7 -Dy1	2.493(2)
O8 -Dy1	2.366(2)
O9 -Dy1	2.329(2)
O10- Dy1	2.411(2)
O1W- Dy1	2.339(2)
O2W- Dy1	2.347(2)
O9 -Dy1 -O2W	77.95(8)
O9- Dy1 -O1W	154.58(7)
O2W -Dy1- O1W	83.49(8)
O9 -Dy1- O8	74.81(7)
O2W-Dy1- O8	143.02(8)
O1W -Dy1 -O8	128.97(7)
O9- Dy1 -O10	116.23(7)
O2W -Dy1- O10	78.60(10)
O1W- Dy1- O10	76.22(8)
O8- Dy1 -O10	91.49(8)
O9 -Dy1- O2	96.05(8)
O2W -Dy1 -O2	127.83(8)
O1W- Dy1- O2	81.71(9)
O8- Dy1 -O2	79.92(7)
O10 -Dy1- O2	143.23(8)
O9- Dy1- O1	85.41(7)
O2W- Dy1 -O1	75.25(8)
O1W -Dy1- O1	73.07(7)
O8- Dy1 -O1	126.12(8)
O10 -Dy1- O1	141.41(8)
O2- Dy1- O1	52.58(7)
O9-Dy1- O7	127.88(7)
O2W -Dy1- O7	147.15(8)
O1W- Dy1- O7	76.19(7)
O8- Dy1 -O7	53.12(7)
O10 -Dy1- O7	71.70(8)
O2- Dy1- O7	74.70(8)
O1- Dy1- O7	121.42(8)
O9- Dy1 -O9	66.22(8)
O2W- Dy1- O9	72.27(7)
O1W- Dy1- O9	124.00(8)
O8 -Dy1- O9	74.08(7)
O10- Dy1- O9	50.24(6)

O2- Dy1- O9	151.52(7)
O1- Dy1- O9	140.38(7)
O7-Dy1-O9	98.09(7)

Table S2. Selected bond lengths for intra- and inter-molecular H-bonding involving hydrogens of water and oxygens of acetate groups.

X-H...Y	X...Y	H...Y	\angle X-H...Y
O1W-H12W...O7 ¹	2.739(2)	1.92	176
O1W-H11W...O1 ²	2.835(2)	2.03	177
O2W-H21W...O10 ³	2.685(2)	1.84	180
C9-H9C...O6 ⁴	3.347(2)	2.46	153

(1) $-x+1/2+1, +y+1/2, +z$ (2) $x, +y-1, +z$ (3) $-x+1/2+1, +y-1/2, +z$ (4) $x-1/2, +y-1, -z+1/2$

Table S3 Best fitted parameters (χ_T , χ_S , τ and α) with the extended Debye model for **1** at 0 Oe in the temperature range 2-7 K.

T / K	$\chi_T / \text{cm}^3 \text{mol}^{-1}$	$\chi_S / \text{cm}^3 \text{mol}^{-1}$	α	τ / s	R ²
2	4.25884	0.32318	0.13526	0.00347	0.99913
2.2	4.0277	0.30648	0.13272	0.00337	0.99914
2.4	3.76853	0.28782	0.13109	0.00325	0.99913
2.6	3.55173	0.27346	0.12942	0.00314	0.99914
2.8	3.35666	0.26154	0.12769	0.00304	0.99913
3	3.18158	0.25056	0.12611	0.00294	0.99913
3.5	2.81514	0.23017	0.12023	0.00267	0.99919
4	2.51788	0.21522	0.11063	0.00236	0.99924
4.5	2.27835	0.20489	0.09619	0.002	0.99927
5	2.06923	0.19515	0.08024	0.0016	0.99955
5.5	1.95545	0.22717	0.05922	0.00126	0.99977
6	1.8053	0.21616	0.04742	9.13359E-4	0.99987
7	1.57089	0.21012	0.03069	4.2403E-4	0.99997

Table S4: Computed energy levels (the ground state is set at zero) and main component of the g -tensor (g_z , transversal components are $g_x = g_y = 0$) for each state for **1** taking into account the dipolar interaction between the Dy centers.

KD	Energy (cm ⁻¹)	g_z
1	0.0	0.00
2	1.0	37.12
3	41.0	0.34
4	41.2	0.34
5	41.7	32.17
6	41.8	32.15
7	81.9	0.00
8	82.7	32.85